



This is a repository copy of *Characterizing the microcirculation of atopic dermatitis using angiographic optical coherence tomography*.

White Rose Research Online URL for this paper:
<http://eprints.whiterose.ac.uk/133308/>

Version: Published Version

Proceedings Paper:

Byers, R.A., Maiti, R., Danby, S.G. orcid.org/0000-0001-7363-140X et al. (6 more authors) (2017) Characterizing the microcirculation of atopic dermatitis using angiographic optical coherence tomography. In: Choi, B., Zeng, H. and Kollias, N., (eds.) Proceedings of SPIE. SPIE BIOS 2017, 28 Jan - 02 Feb 2017, San Francisco, California. Society of Photo-optical Instrumentation Engineers . ISBN 9781510605152

<https://doi.org/10.1117/12.2252407>

© 2017 SPIE. R. A. Byers, R. Maiti, S. G. Danby, E. J. Pang, B. Mitchell, M. J. Carré, R. Lewis, M. J. Cork, S. J. Matcher, "Characterizing the microcirculation of atopic dermatitis using angiographic optical coherence tomography", Proc. SPIE 10037, Photonics in Dermatology and Plastic Surgery, 100370V (6 February 2017); doi: 10.1117/12.2252407. Reproduced in accordance with the publisher's self-archiving policy.

Reuse

Items deposited in White Rose Research Online are protected by copyright, with all rights reserved unless indicated otherwise. They may be downloaded and/or printed for private study, or other acts as permitted by national copyright laws. The publisher or other rights holders may allow further reproduction and re-use of the full text version. This is indicated by the licence information on the White Rose Research Online record for the item.

Takedown

If you consider content in White Rose Research Online to be in breach of UK law, please notify us by emailing eprints@whiterose.ac.uk including the URL of the record and the reason for the withdrawal request.



eprints@whiterose.ac.uk
<https://eprints.whiterose.ac.uk/>

PROCEEDINGS OF SPIE

[SPIDigitalLibrary.org/conference-proceedings-of-spie](https://spiedigitallibrary.org/conference-proceedings-of-spie)

Characterizing the microcirculation of atopic dermatitis using angiographic optical coherence tomography

R. A. Byers, R. Maiti, S. G. Danby, E. J. Pang, B. Mitchell, et al.

R. A. Byers, R. Maiti, S. G. Danby, E. J. Pang, B. Mitchell, M. J. Carré, R. Lewis, M. J. Cork, S. J. Matcher, "Characterizing the microcirculation of atopic dermatitis using angiographic optical coherence tomography," Proc. SPIE 10037, Photonics in Dermatology and Plastic Surgery, 100370V (6 February 2017); doi: 10.1117/12.2252407

SPIE.

Event: SPIE BiOS, 2017, San Francisco, California, United States

Characterizing the microcirculation of atopic dermatitis using angiographic optical coherence tomography.

R. A. Byers^{*a}, R. Maiti^b, S. G. Danby^c, E. J. Pang^c, B. Mitchell^c, M. J. Carré^b, R. Lewis^b, M. J. Cork^c and S. J. Matcher^a.

^a*Department of Electronic and Electrical Engineering, University of Sheffield, S3 7HQ.*

^b*Department of Mechanical Engineering, University of Sheffield, S1 4ET.*

^c*Department of Infection, Immunity & Cardiovascular Disease, University of Sheffield, S10 2RX.*

ABSTRACT

Background and Aim: With inflammatory skin conditions such as atopic dermatitis (AD), epidermal thickness is mediated by both pathological hyperplasia and atrophy such as that resulting from corticosteroid treatment. Such changes are likely to influence the depth and shape of the underlying microcirculation. Optical coherence tomography (OCT) provides a non-invasive view into the tissue, however structural measures of epidermal thickness are made challenging due to the lack of a delineated dermal-epidermal junction in AD patients. Instead, angiographic extensions to OCT may allow for direct measurement of vascular depth, potentially presenting a more robust method of estimating the degree of epidermal thickening.

Methods and results: To investigate microcirculatory changes within AD patients, volumes of angiographic OCT data were collected from 5 healthy volunteers and compared to that of 5 AD patients. Test sites included the cubital and popliteal fossa, which are commonly affected by AD. Measurements of the capillary loop and superficial arteriolar plexus (SAP) depth were acquired and used to estimate the lower and upper bounds of the undulating basement membrane of the dermal-epidermal junction. Furthermore, quantitative parameters such as vessel density and diameter were derived from each dataset and compared between groups. Capillary loop depth increased slightly for AD patients at the popliteal fossa and SAP was found to be measurably deeper in AD patients at both sites, likely due to localized epidermal hyperplasia.

Conclusions: Quantifying subtle changes within vascular morphology and depth may give clinicians an indication of the subsurface abnormalities at both involved and uninvolved AD sites.

Keywords: Optical Coherence Tomography, Angiography, Vivosight, Atopic Dermatitis, Eczema, Speckle Variance.

1. INTRODUCTION

Broadly categorized as a specific form of eczema, atopic dermatitis (AD) is a chronic inflammatory disorder of the skin. Recent US population based studies have estimated the prevalence of the condition at 10.7% for child AD¹ and 10.2% for adult AD², representing a significant quality of life impairment for a substantial portion of the population. Clinical assessment of the extent and severity of AD is typically performed using external grading systems such as the severity scoring of AD³ (SCORAD) or the eczema area and severity index⁴ (EASI) which look for specific signs and coverage of the condition. These externally visible signs often include erythema, edema, papulation, excoriation, lichenification and oozing⁴. There is however substantial evidence that unaffected, lesion-less skin sites of AD patients can remain abnormal, even following remission of the condition⁵. Such "subclinical" abnormalities include epidermal barrier dysfunction characterized by significant differences in trans-epidermal water loss (TEWL), pH and capacitance between healthy and unaffected skin^{6,7} as well as structural abnormalities such as epidermal hyperplasia⁵. Indeed it appears clear that externally healthy looking skin of previously diagnosed AD patients is likely to contain hidden abnormalities beneath the skin surface⁸. Knowledge of such abnormalities could facilitate improved treatments which aim to monitor and suppress progression of the disorder past the point of clinical remission⁵.

*rabyers1@shef.ac.uk (*Biophotonics Group, Kroto Research Institute, Univ of Sheffield, Broad Lane, Sheffield, S3 7HQ*)

Optical Coherence Tomography (OCT) is an established non-invasive medical-imaging technique which utilizes near-infrared light to capture a reflectance profile of the sub-surface layers within skin. Previous studies have utilized the high axial resolution ($\sim 5\text{-}10\mu\text{m}$) of OCT to delineate the dermal-epidermal junction (DEJ) within skin, allowing for automated measurements of epidermal thickness^{9,10}. In the context of AD, measurements of epidermal hypoplasia (Thinning) following corticosteroid treatment have been well documented using both OCT¹¹ and other non-invasive modalities¹². Comparatively, epidermal hyperplasia (Thickening) is more challenging to accurately quantify using simple structural OCT, owing to a reduction in contrast between the epidermal and dermal layers of the skin as the epidermis thickens (Figure 1). We believe this loss of contrast is related to the presence of localized epidermal psoriasiform hyperplasia; which describes the elongation of the rete-pegs/dermal papillae into the dermis/epidermis, a condition previously documented in AD affected skin¹³. The result is a highly oscillatory DEJ of which the epidermal basal cells lie at a range of depths within the tissue. Given such morphology, automated algorithms will generally fail to capture sharp undulations in the DEJ, similarly manual measurements are made increasingly subjective due to the lack of a clearly defined border between the epidermis and dermis. Furthermore, it remains challenging to consistently define epidermal thickness under these conditions, should measurements be made at the tips of the dermal papillae or the deepest points along each rete-peg? Realistically a measure of average epidermal thickness should lie somewhere in between.

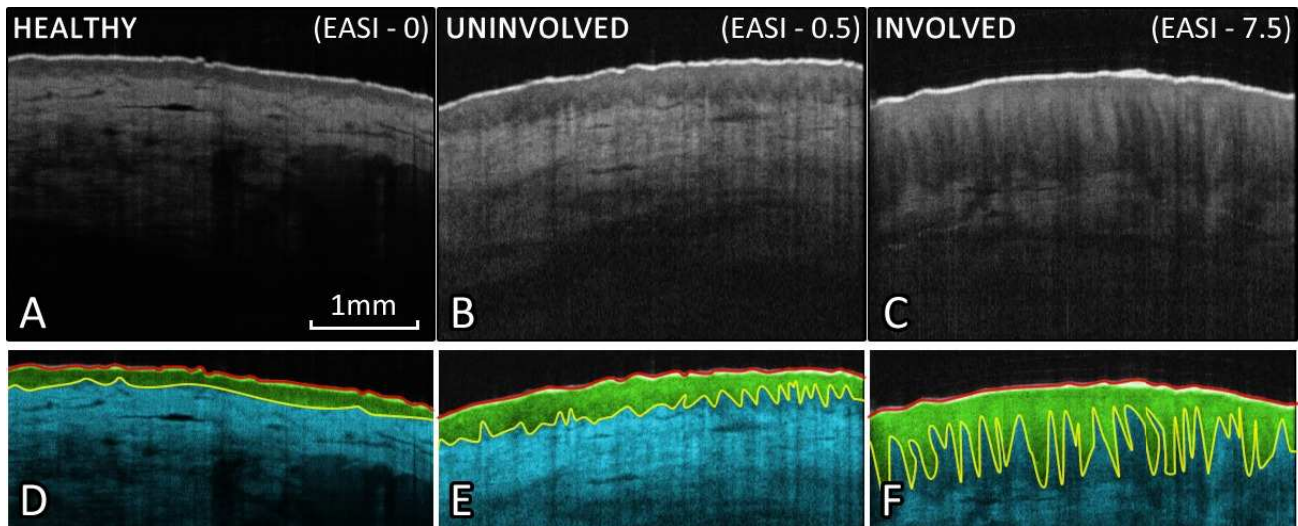


Figure 1. OCT images of the popliteal-fossa highlighting the reduction of DEJ contrast as epidermal hyperplasia increases. A) OCT image captured from a healthy subject (Local EASI = 0), showing clear delineation of the epidermis and dermis. B) OCT image captured from an uninvolved site on an eczema patient, showing slightly extended rete-pegs and an undulating DEJ. C) OCT image captured from an involved site on a different eczema patient, showing what appears to be psoriasiform hyperplasia (Long thin epidermal papillae/rete-pegs). D-F) Manually segmented skin layers. Red line is the skin surface / stratum corneum layer. Green coloration represents the epidermis, Yellow-line is the DEJ and blue coloration represents the dermis.

An alternative method of quantifying the degree of epidermal hyperplasia could be to measure the depth of vascular layers of the skin. Firstly, the superficial arteriolar plexus (SAP) which lies horizontally in the papillary dermis, could be considered a lower bound for the true DEJ location. Secondly, the tips of the capillary loops which extend vertically into each of the dermal papillae represent the thinnest points of the epidermis and could be considered an upper bound for the DEJ location (Figure 2). Furthermore, the density (Loops/ mm^2) and height (mm) of these capillary loops could give some indication as to how “rough” the DEJ is, that is how many times it rises and falls again over a certain area of skin. Recently developed processing methods have enabled the extraction of three-dimensional angiographic data from oversampled structural OCT datasets^{14,15}. One such method, termed speckle-variance OCT (svOCT) identifies the presence of fluid flow by considering the temporal evolution of intensity (speckle) within each pixel of a volume. Pixels in a solid region of tissue exhibit intensities which can be characterized by a Gaussian distribution, due to random acquisition noise. Comparatively, pixels in a fluid region of tissue will exhibit intensities in a Rayleigh distribution, as a

combination of both acquisition noise and moving speckle¹⁶. This gives rise to contrast between solid and fluid regions of the skin. The aim of the study is to explore whether visualization of these underlying micro-vessels can enable less subjective and potentially automated measurements of epidermal hyperplasia to be acquired. In addition, through direct comparison to healthy subjects, we aim to visualize morphological changes within the microcirculation as a result of AD, both at uninvolved and involved sites.

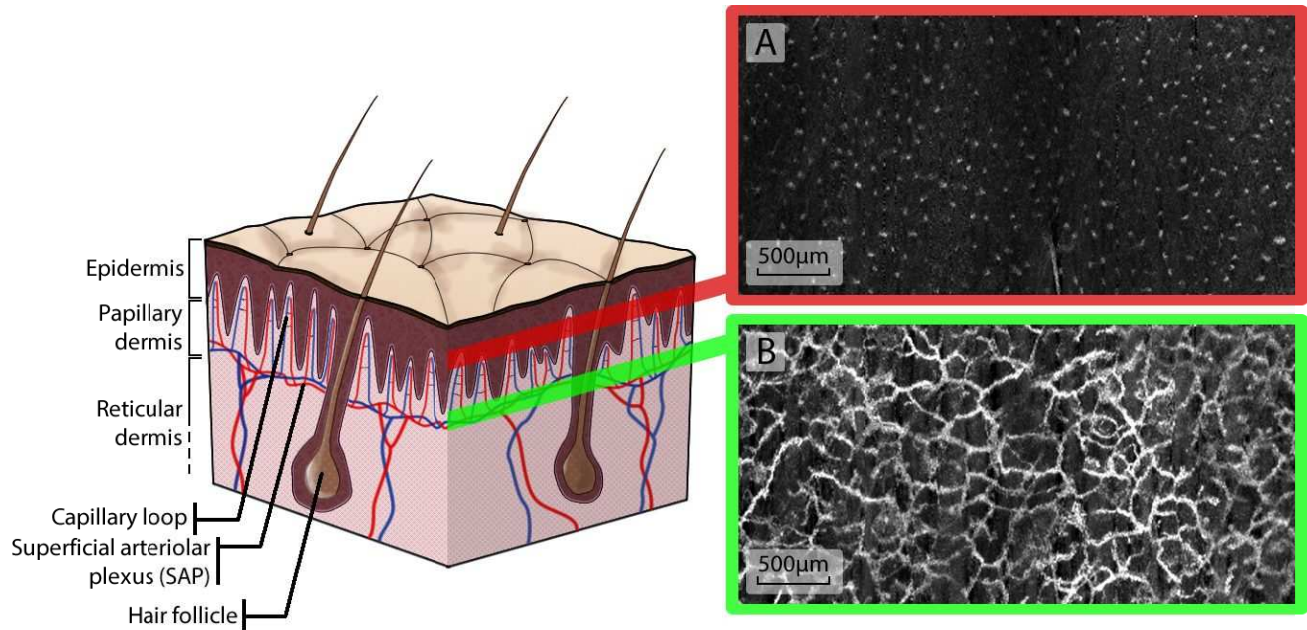


Figure 2. The basic structure of skin affected by psoriasiform hyperplasia (Sebaceous glands and sweat ducts omitted for clarity). Vertical arteries and capillaries rise from the deep arterial plexus and form a horizontal network termed the superficial arteriolar plexus (SAP). From this, capillary loops consisting of both rising arterioles and falling venules form hairpin like structures in the dermal papillae. A) An *en-face* angiographic svOCT image captured at a depth corresponding to the tips of the capillary loops. Visible as small dots in the *en-face* perspective. B) An *en-face* angiographic svOCT image captured at a depth corresponding to the SAP. Large interconnected vessels are visible. The difference in depth between these two layers could be analogous to the height of the rete-pegs.

2. MATERIALS AND METHODS

2.1 Participants

One cohort of 5 volunteers with healthy skin and a second cohort of 5 volunteers with active AD were recruited. Both male and females aged 18-60 with Fitzpatrick skin type I-III (Mexameter melanin reading of <350) were recruited on a first-come first served basis. Inclusion criteria for the healthy cohort included having no prior history of any chronic skin condition. Inclusion criteria for the AD cohort included having currently active AD (As defined by the UK working party diagnostic criteria) as well as having no history of non-AD skin conditions. Exclusion criteria for both groups included the use of any medication (Other than birth control) that could potentially interfere with the study, pregnancy and excessive hair/pigmentation at imaging sites. Informed consent was obtained from each participant prior to imaging and all participants received remuneration for their involvement. The National Research Ethics Service (NRES) Committee East Midlands–Derby, formally known as Trent Multicentre Research Ethics Committee (MREC), approved the study, under the project reference 04/MREC/70.

2.2 Imaging protocol

All imaging for this study was performed using a multi-beam OCT system (Vivosight®, Michelson Diagnostics Ltd, Orpington, Kent, UK) running at 20 kHz line acquisition rate. This system utilizes a swept-source 1305nm Axsun laser

with a bandwidth of 147nm, allowing visualization of structures to a depth of $\sim 500\mu\text{m}$ in skin. Four imaging sites which commonly exhibit AD symptoms were chosen for the study, these being the left and right cubital fossa (inner elbow) as well as the left and right popliteal fossa (inner knee).

Prior to imaging, each participant was asked to wait 10 minutes in the study room with the skin of the test sites exposed, this process aimed to acclimatize each of the test sites such that any homeostatic variance was minimized. Following this, the participant was assessed independently by two different graders in order to establish both regional and local EASI scores based on dryness, erythema, edema/papulation, excoriation and lichenification. The handheld probe of the OCT system was then positioned for imaging using a mechanical clamp, such that any movement artifacts originating from the operator were eliminated. A plastic cap bridged the gap between the OCT probe and the skin, this was deemed necessary in order to reduce any lateral movement of the skin surface during imaging.

Imaging was then performed, with four-dimensional (x - y - z -time) structural OCT volumes being collected from each skin site in turn. These datasets were collected with $10\mu\text{m}$ lateral resolution and $3.9\mu\text{m}$ axial resolution, over a volume of $4\times 4\times 2\text{mm}$; 10 repeat scans were collected at each y -location such that a measure of variance could be calculated for the svOCT methodology. With these settings, the resulting volume was $400\times 400\times 512\times 10$ in size, with each scan taking approximately 80 seconds to acquire and save. The raw data was processed offline in MATLAB (R2014b – MathWorks) into an angiographic format following a previously described methodology¹⁵.

2.3 Quantification of vascular parameters

Capillary loop depth was defined as the depth beneath the skin surface at which the tips of the capillary loops became visible (Figure 2A), this measurement could be considered an upper bound for the average DEJ location. Similarly, SAP depth was defined as the depth at which the majority of capillary loops in the field of view were connected by horizontal vessels (Figure 2B), a measurement which could be considered a lower bound for the average DEJ location. For this study, SAP depth was determined by eye. In future, this could be performed analytically by considering the connectedness of the capillary loops.

Further vessel parameters were derived through direct quantification of mean-intensity projection images captured over a wide-depth range (30 - $300\mu\text{m}$) within the tissue. Figure 3 shows the steps that were taken in order to skeletonize the data.

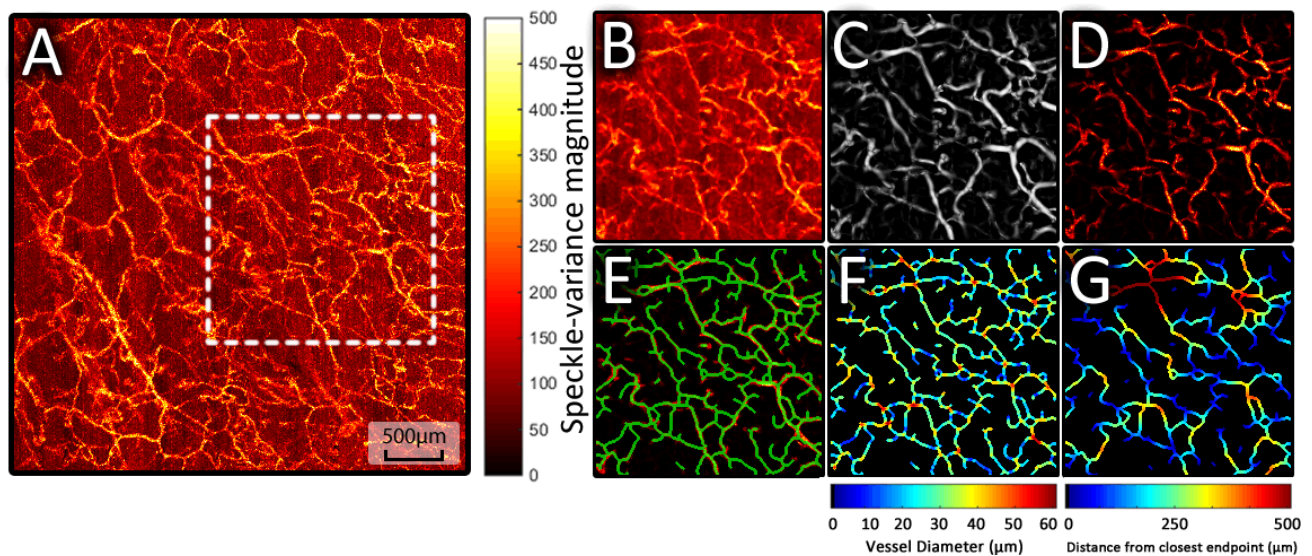


Figure 3. Steps taken to skeletonize and quantify vascular parameters from both healthy and AD datasets. A) *En-face* mean intensity projection captured from the popliteal fossa site of a healthy participant. White box shows the FOV used for B-G. B) Median filtering step. C) "Frangi" vesselness filtering. D) Result of masking B with the vesselness data in C. E) Resulting skeleton (Green) overlaid on the masked data. F) Measured vessel diameter at each point along the vessel. G) Measured distance to the closest skeleton endpoint at each point along the vessel.

Briefly, the data was first median filtered to remove noise. A "Frangi" vessel enhancement filter¹⁷ was then applied, this filter detects and highlights tubular regions of an image through consideration of the eigenvalues of the Hessian matrix. This filtered image was then used to compose a mask for the original data, preserving only areas which were likely to be vascular. These filtering steps were deemed necessary due to the large magnitude of svOCT background noise, some of which is derived from movement of the participant during imaging. Following these steps, the image was binarized using an automatically detected threshold (Otsu's method), with the binary image then being used to generate a vessel skeleton.

Four quantitative parameters were extracted using both the binarized data together with the vascular skeleton. Average vessel diameter (μm) was defined as double the average distance from the skeleton to the closest zero in the binarized image. Average path length (μm) was a measure of connectivity in the image, and was calculated as the average path distance (Tracing the skeleton) from each end-point to its furthest connected neighbor. Vessel density (%) was defined as total vascular coverage across the region while total vessel length per unit area (mm^{-1}) was calculated by dividing the total length of vessels in the image by the size of the area (16mm^2).

3. RESULTS AND DISCUSSION

Figure 4 shows a selection of 3D angiographic datasets from both the healthy and AD participants at each unique skin site. These images are color-coded according to depth beneath the skin surface, hence vessels with red coloration lie between 39 and 117 μm , vessels with green coloration lie between 117 and 195 μm and vessels with blue coloration lie between 195 and 273 μm .

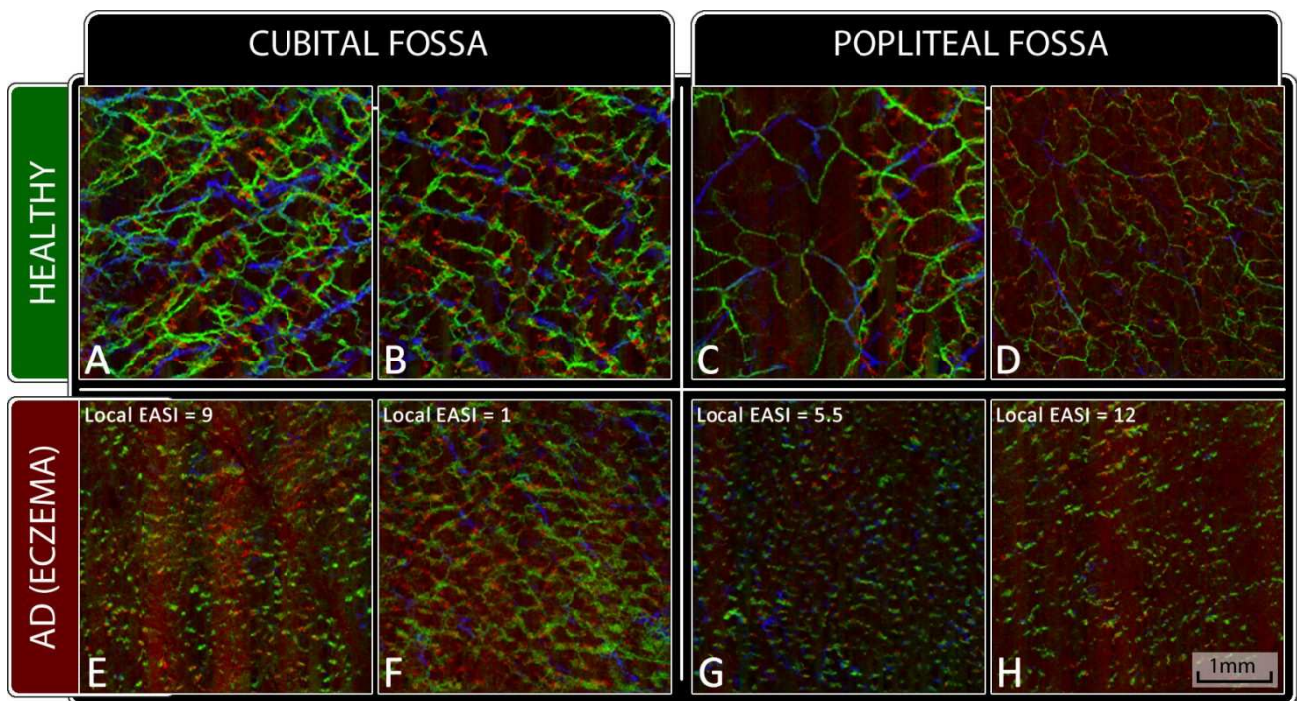


Figure 4. A selection of *en-face* angiography images captured from both healthy and AD participants at both skin sites. Images are color-coded for depth such that red coloration is for superficial vessels (39-117 μm), green for mid-depth vessels (117-195 μm) and blue for deeper vessels (195-273 μm). All images are 4x4mm.

For both healthy and AD participants, capillary loops were visible as small red dots in the *en-face* perspective. For healthy participants, a horizontal plexus was also visible with the majority of vessels having a green coloration (117-195 μm depth). The deep blue vessels which are visible on figure 4 panels A, B, C, D, F and G are potentially the large vessels which descend into the reticular dermis. One primary distinction in certain AD participants was the lack of a

visible SAP over the depth range displayed here (39-273 μm) as seen in figure 4E, G and H, this is a result of the SAP being even deeper into the tissue as shown on figure 5. Interestingly, many of the AD scans with a low measured local EASI score (<3.5) displayed a SAP depth within the healthy range but the vessels appeared less clearly defined than those in the healthy cohort, as seen on figure 4F. This could be an indication of abnormal flow characteristics within these vessels. Previous studies have shown that while the rheological properties of blood within patients with mild AD stays close to normal¹⁸, the flow rate is significantly reduced at unaffected sites while being significantly raised at acute lesions¹⁹. Slower blood flow could potentially lead to a lower degree of decorrelation for the svOCT protocol, leading to fainter, less defined vasculature as seen here.

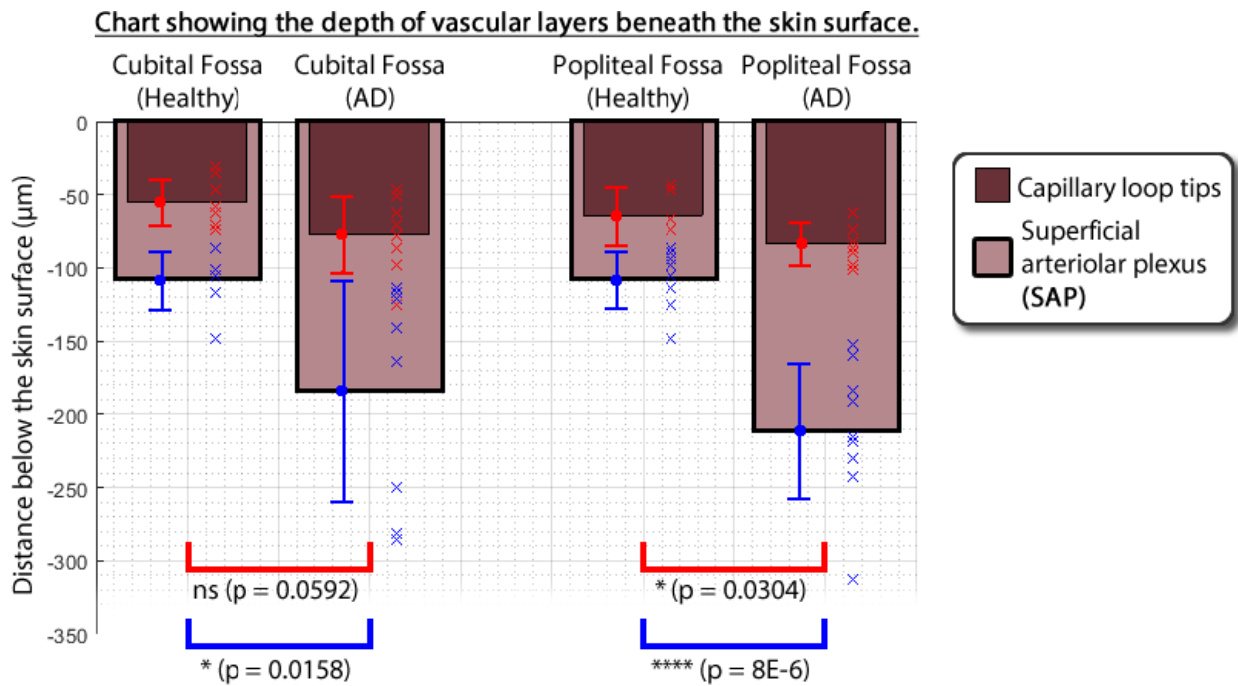


Figure 5. Measured capillary loop and SAP depth beneath the skin surface across the entire dataset. P-values calculated using a two-sampled (Unpaired) t-test.

Figure 5 shows the results of manual capillary loop and SAP depth measurements for both the healthy and AD cohorts. At the cubital fossa skin site, there was no significant change in the mean capillary loop depth between healthy and AD participants. However at the popliteal fossa site the mean capillary loop depth was significantly deeper for the AD cohort (-19.0 μm). As expected, the measured mean SAP depth was significantly deeper in AD participants at both the cubital fossa (-75.7 μm) and popliteal fossa (-104.0 μm) skin sites. Measured values of both capillary loop depth (-55 μm) and SAP depth (-108 μm) at the healthy cubital fossa were in the range of previously reported values for the healthy forearm (Reported as -68 μm and -116 μm respectively)¹², suggesting the modality is capable of accurately detecting these layers. Overall these results confirm that as expected, the SAP is pushed deeper into the tissue as a consequence of epidermal psoriasisiform hyperplasia. Care must be taken when measuring the thickness of the epidermis, as the DEJ does not lie flat in areas affected by AD, as evidenced by the large distance between the capillary loop depth and the SAP depth.

Figure 6 shows how the automatically measured parameters detailed in section 2.3 varied with skin site and the presence of AD. For the cubital fossa there was no change in the average vessel diameter between cohorts, while a significant increase in vessel diameter was measured in participants with AD at the popliteal fossa. For an inflammatory condition such as AD, one might expect the capillaries to dilate and thus have a measurably higher diameter at both locations. One reason why this may not be apparent at the cubital fossa site is due to healthy patients having a measurably higher vessel density, it could be that vessels lying in close proximity or even crossing above or beneath the vessel in question are being anomalously merged together during the binarization step. It may be beneficial for future work to take vessel depth

Charts showing the variance of automatically acquired quantitative parameters as a function of skin site and AD presence.

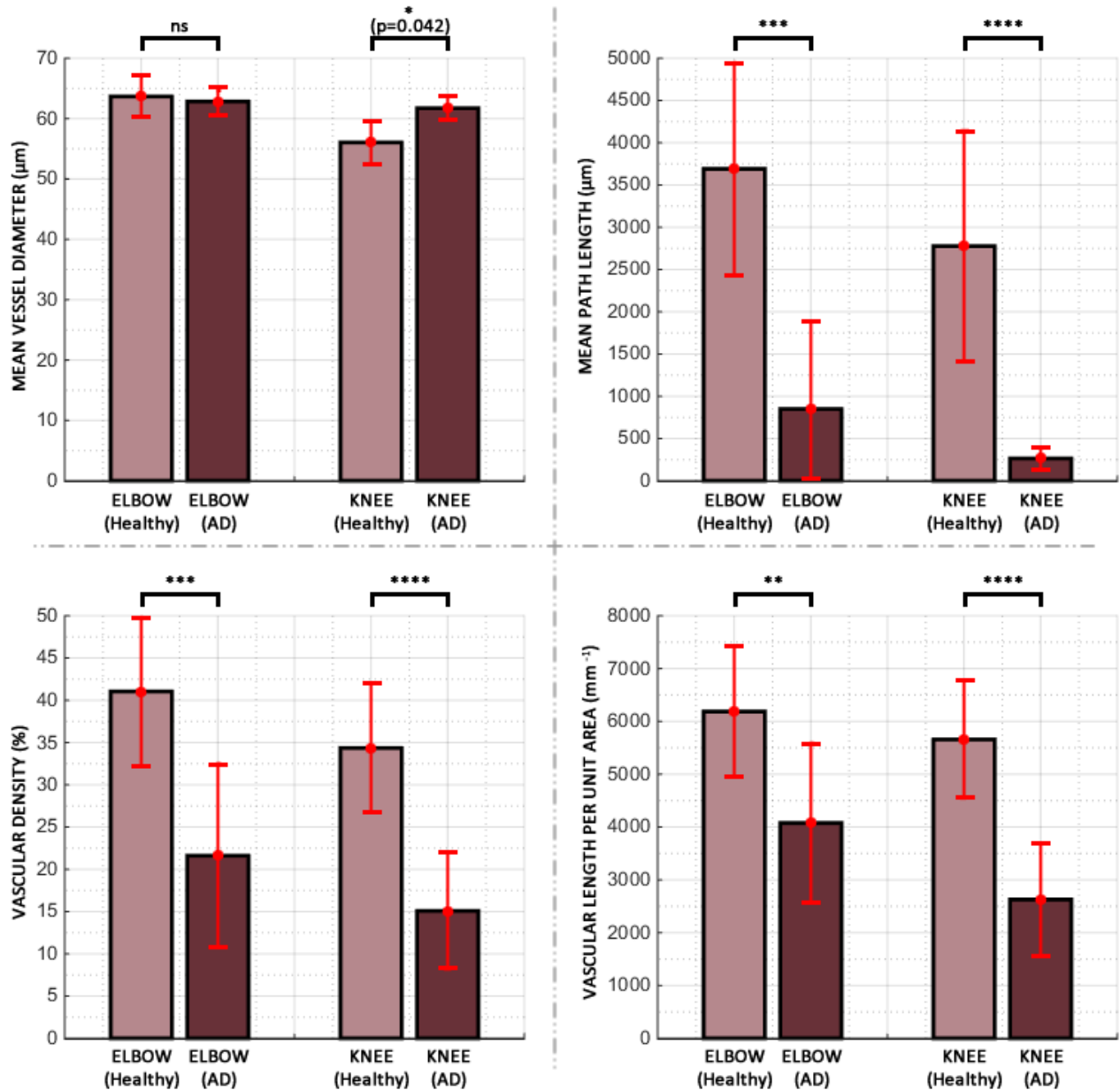


Figure 6. Charts showing the variance of quantitative parameters which were automatically extracted from the datasets following the binarization and skeletonization steps outlined in section 2.3. (** = $P \leq 0.01$, *** = $P \leq 0.001$, **** = $P \leq 0.0001$).

into consideration, segmenting the vessels into numerous sub-layers such that overlapping vessels are not merged.

Significant reductions in mean path length, mean vascular density and mean vascular length per unit area were observed for the AD participants at both skin sites. Lower mean path length is representative of the lack of connectivity between the vessel structures in the skin of the AD participants, particularly at the cubital fossa sites where the SAP depth was $>200\mu\text{m}$ (Figure 5) it's very likely that vessel linkages between the capillary loops would occur beneath the penetration depth of the OCT system. The result is a highly segmented skeleton, compared to that of the highly connected skeletons

of the healthy datasets. Similarly, reductions in vascular density and vascular length per unit area are likely to be a direct result of the epidermal hyperplasia, physically pushing a large amount of the vessels out of the field of view of the OCT system. Usage of OCT systems with higher depth penetration than the one used here may allow measurements of capillary loop and SAP depth to be fully automated through utilization of these automatically extracted parameters, for example the location of the SAP could be standardized as the depth at which the connectivity or mean path-length of the volume reaches a certain threshold.

4. CONCLUSIONS

Measurement of vascular parameters within the skin of AD patients can be used as an alternative method of quantifying the degree of epidermal psoriasiform hyperplasia. This is potentially more robust than structural measurements of epidermal thickness as structural contrast is rapidly lost due to sharp undulations in the DEJ, causing automatic measurements to fail and manual measurements to become increasingly subjective. The combination of capillary depth and SAP depth give a reasonable upper and lower bound to the true DEJ location. In future, measurements of capillary loop density could also give some indication to how many rete-pegs are contained within a region.

Overall we can conclude that angiographic svOCT is likely to be a useful tool when monitoring the progression of eczema, particularly once the condition has passed the point of clinical remission but is likely to still exhibit hidden subsurface abnormalities.

5. ACKNOWLEDGEMENTS

This research was supported by BBSRC grant: BB/F016840/1, with equipment funded by MRC grant: MR/L012669/1.

REFERENCES

1. Shaw, T. E., Currie, G. P., Koudelka, C. W. & Simpson, E. L. Eczema Prevalence in the United States: Data from the 2003 National Survey of Children's Health. *J. Invest. Dermatol.* **131**, 67–73 (2011).
2. Silverberg, J. I. & Hanifin, J. M. Adult eczema prevalence and associations with asthma and other health and demographic factors: A US population-based study. *J. Allergy Clin. Immunol.* **132**, 1132–1138 (2013).
3. Severity scoring of atopic dermatitis: the SCORAD index. Consensus Report of the European Task Force on Atopic Dermatitis. *Dermatology* **186**, 23–31 (1993).
4. Hanifin, J. M. *et al.* The eczema area and severity index (EASI): assessment of reliability in atopic dermatitis. EASI Evaluator Group. *Exp. Dermatol.* **10**, 18 (2001).
5. Tang, T. S., Bieber, T. & Williams, H. C. Are the concepts of induction of remission and treatment of subclinical inflammation in atopic dermatitis clinically useful? *J. Allergy Clin. Immunol.* **133**, 1615–1625.e1 (2014).
6. Seidenari, S. & Giusti, G. Objective assessment of the skin of children affected by atopic dermatitis: a study of pH, capacitance and TEWL in eczematous and clinically uninvolved skin. *Acta Derm. Venereol.* **75**, 429–33 (1995).
7. Gupta, J. *et al.* Intrinsically defective skin barrier function in children with atopic dermatitis correlates with

- disease severity. *J. Allergy Clin. Immunol.* **121**, 725–730.e2 (2008).
8. Suárez-Fariñas, M. *et al.* Nonlesional atopic dermatitis skin is characterized by broad terminal differentiation defects and variable immune abnormalities. *J. Allergy Clin. Immunol.* **127**, 954–964.e4 (2011).
 9. Maiti, R. *et al.* In vivo measurement of skin surface strain and sub-surface layer deformation induced by natural tissue stretching. *J. Mech. Behav. Biomed. Mater.* **62**, 556–569 (2016).
 10. Delacruz, J., Weissman, J. & Gossage, K. Automated measurement of epidermal thickness from optical coherence tomography images using line region growing. in (Kollias, N. *et al.*) 75480E (2010). doi:10.1117/12.842353
 11. Lu, Z., Boadi, J., Danby, S., Cork, M. & Matcher, S. J. Optical coherence tomography demonstrates differential epidermal thinning of human forearm volar skin after 2 weeks application of a topical corticosteroid vs a non-steroidal anti-inflammatory alternative. **8565**, 85650C (2013).
 12. Kolbe, L., Kligman, a M., Schreiner, V. & Stoudemayer, T. Corticosteroid-induced atrophy and barrier impairment measured by non-invasive methods in human skin. *Skin Res. Technol.* **7**, 73–77 (2001).
 13. Mihm, M. C., Soter, N. A., Dvorak, H. F. & Austen, K. F. The Structure Of Normal Skin And The Morphology Of Atopic Eczema. *J. Invest. Dermatol.* **67**, 305–312 (1976).
 14. Mariampillai, A. *et al.* Speckle variance detection of microvasculature using swept-source optical coherence tomography. *Opt. Lett.* **33**, 1530–2 (2008).
 15. Byers, R. A., Tozer, G., Brown, N. J. & Matcher, S. J. High-resolution label-free vascular imaging using a commercial, clinically approved dermatological OCT scanner. in (Choi, B. *et al.*) 96890M (2016). doi:10.1117/12.2212222
 16. Lam, E. Y. & Goodman, J. W. A mathematical analysis of the DCT coefficient distributions for images. *IEEE Trans. Image Process.* **9**, 1661–6 (2000).
 17. Frangi, A. F., Niessen, W. J., Vincken, K. L. & Viergever, M. a. Multiscale vessel enhancement filtering. *Medial Image Comput. Comput. Intervention - MICCAI'98. Lect. Notes Comput. Sci. vol 1496* **1496**, 130–137 (1998).
 18. Kasperska-Zajac, A. *et al.* Blood Rheological Properties in Patients with Atopic Dermatitis (AD). *Inflammation* **32**, 242–246 (2009).
 19. Bystryń, J. C. & Hyman, C. Skin blood flow in atopic dermatitis. *J. Invest. Dermatol.* **52**, 189–92 (1969).